Supporting Information

Tunable, colorimetric DNA-based pH sensors mediated by A-motif formation

Sonali Saha,[†] Kasturi Chakraborty,[†] and Yamuna Krishnan*[,†]

[†] National Centre for Biological Sciences, Tata Institute of Fundamental Research, GKVK, Bellary Road, Bangalore 560 065, India

1. Materials

HPLC purified 5′ thiol modified oligonucleotides were purchased from IBA GmbH, Germany. Hydrogen tetrachloroaurate(III) ($HAuCl_4.3H_2O$) and tri-Sodium citrate dihydrate ($Na_3C_6H_5O_7{\cdot}2H_2O$), 99%, were purchased from S. D. Fine Chemicals Limited, India. Dithiothreitol (DTT), Sephadex G-25 (DNA grade) and all other reagents were purchased from Sigma-Aldrich, USA. 96 well tissue culture plates for colorimetric assays were purchased from Tarsons, India. Milli-Q water was used for all experiments.

2. Instrumentations

Gold nanoparticle (GNP) solutions and oligonucleotides were quantified using Cary 300 bio UV-Visible Spectrophotometer, Agilent Technologies in 1 cm quartz cuvette. UV-vis absorption spectra for colorimetric assay were recorded from 400 nm to 800 nm using SpectraMax M5 Multimode Microplate reader, Molecular Devices.

3. Preparation of GNPs

13 nm GNPs were synthesized by the citrate reduction method described previously.[1] Briefly, 20 mL of 1 mM $HAuCl_4$ aqueous solution was heated to 60^{o} C with constant stirring. 2 mL of 38.8 mM sodium citrate was added rapidly at a time, and then the solution was refluxed for an additional 30 min while stirring vigorously. The color changed from pale yellow to deep red, and the solution was allowed to cool to room temperature before use. Size of the GNPs (13.2 ± 1.55 nm) was determined from TEM images confirms the synthesis of monodisperse GNPs (data not shown). The concentrations of 13 nm GNPs were determined using UV-vis spectroscopy (extinction coefficient: 2.7×10^8 M^{-1} cm^{-1} at λ_{520} for 13 nm GNPs).[2]

4. Preparation of oligonucleotide modified GNPs

GNPs were functionalized with oligonucleotides using modified literature methods.[3] Briefly, the disulfide bonds between the oligonucleotides were reduced prior to GNP functionalization by DTT treatment. DTT treatment was done using 100 fold molar excess DTT over oligonucleotides (total 25 μM), in presence of 5 mM TE buffer of pH 8 (10 mM Tris-Cl, pH 8 and 1 mM EDTA) for 1 h at room temperature. The reduced oligonucleotides were purified using a spin column packed with Sephadex G-25 column and then immediately added to an aqueous solution of GNPs (3 nmol of oligonucleotide/mL GNPs). 10 fold molar excess of spacer oligonucleotides compared to A-rich oligonucleotides have been used for GNP modification. The oligonucleotide added GNP solution was allowed to incubate with constant shaking overnight at room temperature. To remove excess oligonucleotides, the GNPs were centrifuged at 13,000 rpm for 30 min at 4^{o} C. The supernatant was removed, leaving a pellet of gold nanoparticles at the bottom of an Eppendorf tube. The particles then were resuspended in Milli Q water and stored at 4^{o} C.

5. Spacer oligonucleotides

Incorporation of 10 fold molar excess of spacer oligonucleotides prevents the formation of "intraparticle" A-motifs (i.e., A-motifs formed from proximal A-rich oligonucleotides on the surface of the same GNP, Fig. S4 (I)) as well as minimize surface crowding during the formation of "interparticle" A-motifs. The electrostatic repulsion between the A_{30} backbone and the negatively charged S_6 shell on the GNP would inhibit intraparticle A-motif formation. According to the design shown in Scheme 1 in main text, the spacer length on GNPs determines the effective thickness of the negatively charged shell on the GNP surface.

6. Colorimetric assay

3 nM A_n-S_m functionalized GNPs were incubated in 10 mM buffers of different pH ranging from pH 2 to 7. The solutions were incubated for 15 min at room temperature before data acquisition. Analysis of these solutions by UV-Vis spectroscopy revealed that at higher pH, absorbance at 520 nm characteristic of isolated GNPs was observed, while at acidic pH the 520 nm peak shifted to higher wavelengths and a new, broad absorption (540–750 nm) appeared for aggregated GNPs. In brief, the bathochromic shift of GNP absorbance correlated perfectly with decreasing pH value of the solutions in Fig. 1A (main text). Upon GNP aggregation, their absorbance at 700 nm (A_{700}) intensified and the Plasmon absorbance at 520 nm (A_{520})

corresponding to individual GNPs decreased. Thus the extent of color change corresponding to extent of aggregation is revealed from the absorbance ratio (A_{520}/A_{700}) that is a quantitative representation of the color of the system.[4] In these experiments, the solutions were agitated each time before recording optical spectra to ensure homogeneity of the particle suspension.

7. Mutational analysis

From the positional mutation analysis data (Fig. 2A, main text), we observe that the A residues at the exposed 3′ end is most important in mediating interparticle A-motif formation. Notably, this is in contrast to duplex DNA where hybridization happens in a head to tail orientation and mutations at the centre of the duplex cause the greatest destabilization.[5] This can be reconciled from the difference between the mechanisms of B-DNA and A-motif duplexation. The former needs a 'seed' complementary region that functions as a nucleating region and finally zips up to form the double helix,[6] whereas A-motif formation is diffusion controlled, with every collision being a productive one, leading to a 'creeping' mechanism that results in complete base pairing.[7]

8. Mutational analysis supports the 'fold-back' mode of association

In order to probe interparticle GNP association in case of A_{30}-S_6 GNP, we chose GNPs modified with A-rich oligonucleotides of constant length (30 mer), but incorporating A→T mutations at specific positions that could result in a mismatch at a pre-designated locations (shown in Table 1) in the expected fold-back A-motif or head-to-head A-motif. We chose the residues on dA_{30} for mutation corresponding to four distinct regions on the expected 'fold-back' A-motif model (Fig. S1A). These were (i) **B1:** residues involved in intramolecular AH^+-H^+A base pairing (shown in magenta), (iii) $\mathbf{T_d}$**:** residues present at the turn, distal from the GNP surface and potentially available for interparticle AH^+-H^+A base pairing (shown in orange), (iv) $\mathbf{T_p}$**:** residues present at the turn, proximal to the GNP surface and therefore unavailable for AH^+-H^+A base pairing *only in the case of fold-back structure* (shown in dark blue) and (v) **L1:** residues in the loop (shown in red) (Fig. S1A) also unavailable for AH^+-H^+A base pairing *only in the case of fold-back structure*. Residues on dA_{30} buried in the spacer shell surrounding the GNP were not considered for mutation (cyan region).

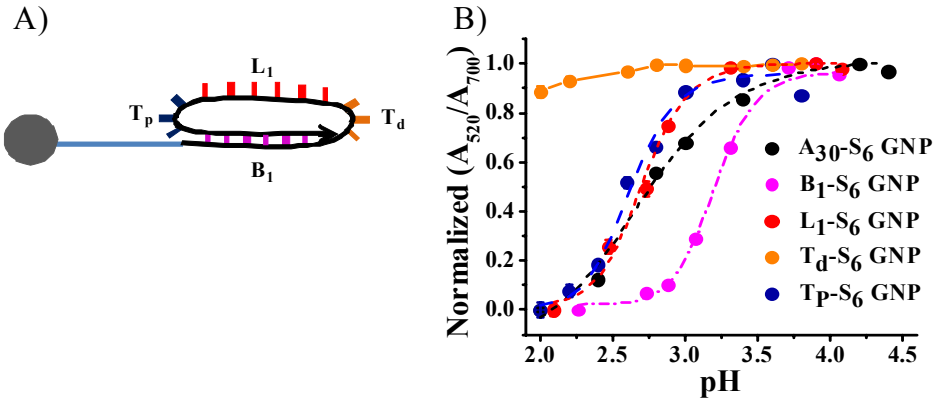

Figure S1 (A) Working model for proposed 'fold-back' A-motif. 5′ residues buried in the spacer oligos are shown in light blue. Four distinct regions on the expected 'fold-back' A-motif model have been indicated as B_1: magenta; T_d: orange; L_1: red and T_p: dark blue. Mutated residues have been shown as bold lines. (B) Comparison of the normalized curves of the colorimetrically quantified pH dependent interparticle association of the GNPs modified with dA_{30} carrying A→T mutations at the positions shown in (A).

In case of interparticle GNP association via 'head-to-head' hybridization, all the mutated dA_{30} sequences are expected to show shift in $pH_{1/2}$ towards lower pH values due to destabilization of the resultant interparticle A-motifs. Fig. S1B shows the corresponding sigmoidal transition curves. Mutations at various positions on dA_{30} show different effects on interparticle association which indicates differential accessibility of these residues for interparticle AH^+-H^+A base pairing. As expected, the pH response of L_1-S_6 GNPs remain constant compared to A_{30}-S_6 GNPs, characteristic of either (i) mutations in the centre of A-rich tracts having no effect in a head-to-head mode of association or (ii) no effect of these residues in the stability of a fold-back A-motif model (as seen in Fig. S1A) due to their non-interacting nature in the fold-back loop. In the head-to-head model of interparticle association, A→T mutations on B_1-S_6 GNPs should show a *decrease* in $pH_{1/2}$ values. However, these showed a $pH_{1/2}$ that was substantially shifted towards higher pH values. This may be explained by the greater destabilization caused to the AH^+-H^+A base pairs in the fold-back A-motif. This decrease in fold-back A-motif stability, would lead to a greater proportion of interparticle association mediated by a greater proportion of A-rich strands associating via the head-to-head mode which is expected to have higher $pH_{1/2}$ values (Fig. 3B revised manuscript). Consistent with this, T_d-S_6 GNPs shows a dramatic decrease in $pH_{1/2}$ compared to the native A_{30}-S_6 GNP, indicating crucial involvement of these residues in mediating interparticle GNP association. Importantly in a linear,

head-to-head A-motif model, mutations in this region should show *negligible* change in $pH_{1/2}$ (similar to L1-S6 GNPs). This strongly supports that the A-tract has folded back, leaving these residues at the distal terminus, that can promote interparticle GNP association by further AH^+-H^+A base pairing. In perfect accordance, T_p-S_6 GNP particles showed negligible change in their pH response compared to A_{30}-S_6 GNP. Taken together, these mutational data support a model of 'fold-back' A-motif mediated association as shown in Fig. 3C. Importantly, the data in Fig. 3A & 3B (main text) do not fit a model of a simple unimodal association, i.e., head-to-head hybridization alone by long poly dA tracts, although this is true for short poly dA tracts.

9. Table showing buffers of different pH ranges:

pH range	Buffers
2.0 – 4.2	Citrate
4.2 – 5.5	Acetate
5.5 – 7.0	Phosphate

References:

(1) J. J. Storhoff, R. Elghanian, R. C. Mucic, C. A. Mirkin and R. L. Letsinger, *J. Am. Chem. Soc.*, 1998, **120**, 1959.

(2) F. Huo, A. K. R. Lytton-Jean and C. A. Mirkin, *Adv. Mater.*, 2006, **18**, 2304.

(3) S. J. Hurst, A. K. R. Lytton-Jean and C. A. Mirkin, *Anal. Chem.*, 2006, **78**, 8313.

(4) J. Liu and Y. Lu, *J. Am. Chem. Soc.*, 2003, **125**, 6642.

(5) Z. Guo, Q. Liu and L. M. Smith, *Nat. Biotechnol.*, 1997, **15**, 331.

(6) C. Sönnichsen, B. M. Reinhard, J. Liphardt and A. P. Alivisatos, *Nat. Biotechnol.*, 2005, **23**, 741.

(7) R. Maggini, F. Secco, M. Venturini and H. Diebler, *Faraday Trans.*, 1994, **90**, 2359.

(8) S. Chakraborty, S. Sharma, P. K. Maiti and Y. Krishnan, *Nucleic Acids Res.*, 2009, **37**, 2810.

Name of the oligonucleotide	Sequences (5′ to 3′) All the sequences contain 5′ thiol modification
A_8	AAAAAAAA
A_{15}	AAAAAAAAAAAAAAA
A_{22}	AAAAAAAAAAAAAAAAAAAAAA
A_{30}	AAAAAAAAAAAAAAAAAAAAAAAAAAAAAA
T_{15}	TTTTTTTTTTTTTTT
S_6	ATTATA
S_9	CGATATATT
S_{12}	CGATATCTTCGT
S_{15}	CGATATCTTCGTTAT
S_{18}	GAACCACGATATCTTCGT
S_{21}	GAACCACGATATCTTCGTTAT
S_{24}	CTCGAACCACGATATCTTCGTTAT
S_{28}	GCGACTGATGGCGAGTGCAAAGCGTGGC
M_1	AAAAAAAAAAA***T***AAA
M_5'	AAAAA***T***AAAAAAAAA
M_3'	AAAAAAAAAAAAAA***T***
M_2	AAAAAAAA***T***AA***T***AAA
M_3	AAAAAAAA***T***AA***T***AA***T***
B_1	AAAAAAAA***T***A***T***AAAAAAAAAAAAAAAAAAA
L_1	AAAAAAAAAAAAAAAA***T***AA***T***AAAAAAAAAA
T_d	AAAAAAAAAAAAAAAAAAAA***TT***AAAAAAA
T_p	AAAAAAAAAAAAA***TT***AAAAAAAAAAAAAAA

Table S1 The sequences of the 5′ thiol modified oligonucleotides for GNP modification. Bases shown in bold and italics represent mutated sites that would result in mismatches in the corresponding A-motif.

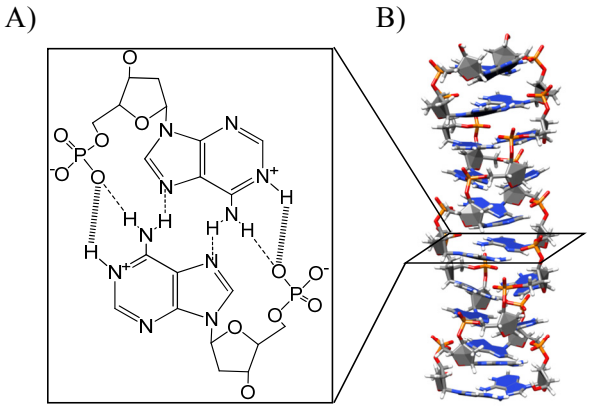

Figure S2 (A) Shows the AH^+-H^+A base pairing scheme in A-motif. (B) N1-protonated adenosine mediated parallel duplex of A-motif (Adapted from ref 8).

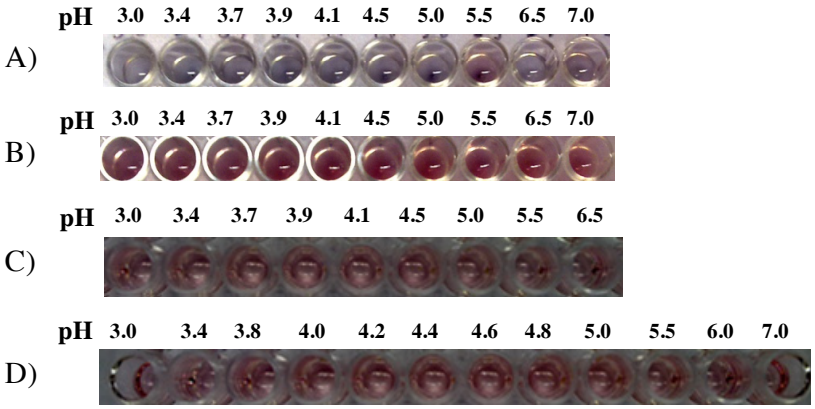

Figure S3 Control experiments showing negligible color changes of solutions containing unmodified GNPs (A); S_6 modified GNPs (B); T_{15}-S_6 modified GNPs (C) and A_{15}-S_{28} modified GNPs (D) as a function of pH. These color changes are quantified and presented in **Figure 1B** of the main text.

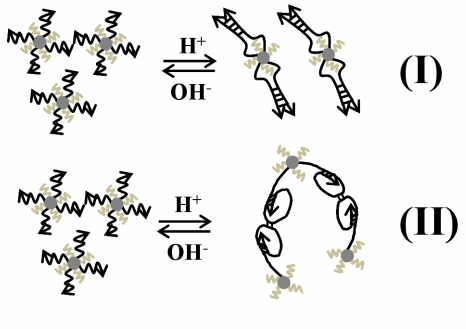

Figure S4 Schematic illustrating the proposed mechanisms to explain the discrepancy of transition pH ($pH_{1/2}$) shown by A_{30}-S_6.

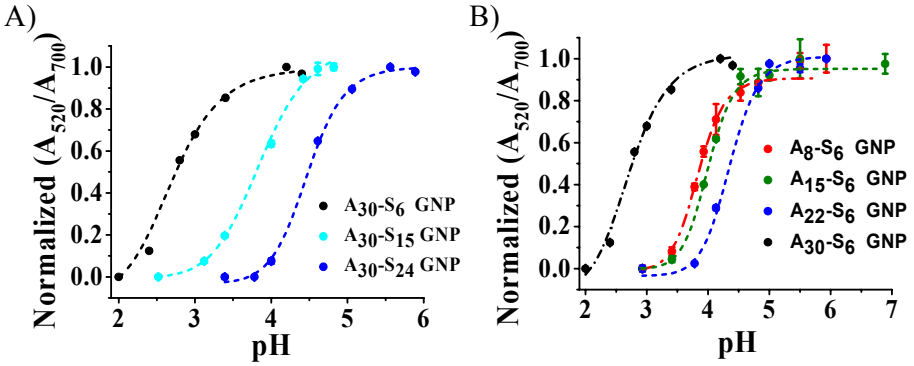

Figure S5 Comparison of the normalized curves of the colorimetrically quantified pH dependent interparticle association of the GNPs (A) modified with dA_n (where n= 8, 15, 22 and 30) and dS_6. (B) modified with dA_{30} and dS_m (where m= 6, 15, and 24). Interparticle associations are quantified by the ratios of UV-vis absorption (A_{520}/A_{700}) as a function of pH.

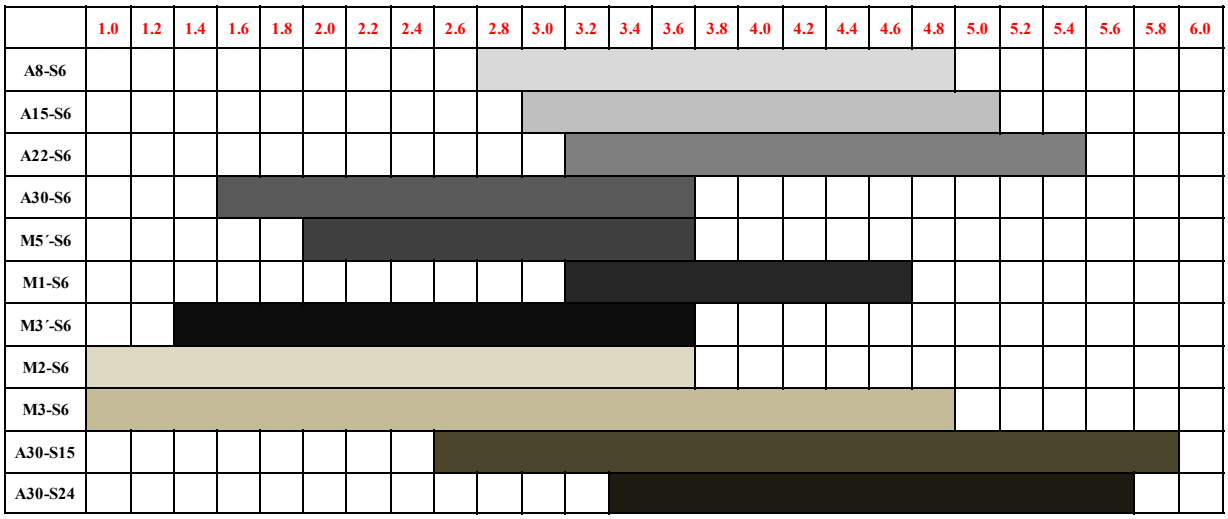

Table S2 Shows tunable pH sensitive range of differentially modified GNPs as colorimetric sensor. Top most row indicates pH and left most column indicates the GNP modifications.